

Vector solitons with locked and precessing states of polarization

Sergey V. Sergeyev,* Chengbo Mou, Aleksey Rozhin, and Sergei K. Turitsyn

Aston Institute of Photonic Technologies, School of Engineering & Applied Science Aston University, Birmingham, B4 7ET, UK

*sergey.sergeyev@gmail.com

Abstract: We demonstrate experimentally new families of vector solitons with locked and precessing states of polarization for fundamental and multipulse soliton operations in a carbon nanotube mode-locked fiber laser with anomalous dispersion laser cavity.

©2012 Optical Society of America

OCIS codes: (060.3510) Lasers, fiber; (140.4050) Mode-locked lasers; (250.5530) Pulse propagation and temporal solitons.

References and links

1. G. D. VanWiggeren and R. Roy, "Communication with dynamically fluctuating states of light polarization," *Phys. Rev. Lett.* **88**(9), 097903 (2002).
2. L. Tong, V. D. Miljković, and M. Käll, "Alignment, rotation, and spinning of single plasmonic nanoparticles and nanowires using polarization dependent optical forces," *Nano Lett.* **10**(1), 268–273 (2010).
3. M. Spanner, K. M. Davitt, and M. Y. Ivanova, "Stability of angular confinement and rotational acceleration of a diatomic molecule in an optical centrifuge," *J. Chem. Phys.* **115**(18), 8403–8410 (2001).
4. N. Kanda, T. Higuchi, H. Shimizu, K. Konishi, K. Yoshioka, and M. Kuwata-Gonokami, "The vectorial control of magnetization by light," *Nat Commun* **2**, 362 (2011).
5. S. V. Sergeyev, "Spontaneous Light Polarization Symmetry Breaking for an anisotropic ring cavity dye laser," *Phys. Rev. A* **59**(5), 3909–3917 (1999).
6. H. Zeghlache and A. Boulnois, "Polarization instability in lasers. I. Model and steady states of neodymium-doped fiber lasers," *Phys. Rev. A* **52**(5), 4229–4242 (1995).
7. R. Leners and G. Stéphan, "Rate equation analysis of a multimode bipolarization Nd³⁺ doped fibre laser," *Quantum Semiclass. Opt.* **7**(5), 757–794 (1995).
8. Yu. V. Loiko, A. M. Kul'minskii, and A. P. Voitovich, "Impact of the vectorial degrees of freedom on the nonlinear behavior of class B lasers," *Opt. Commun.* **210**(1-2), 121–148 (2002).
9. G. D. Van Wiggeren and R. Roy, "High-speed fiber-optic polarization analyzer: measurements of the polarization dynamics of an erbium-doped fiber ring laser," *Opt. Commun.* **164**(1-3), 107–120 (1999).
10. S. Sergeyev, K. O'Mahoney, S. Popov, and A. T. Friberg, "Coherence and anticohere resonance in high-concentration erbium-doped fiber laser," *Opt. Lett.* **35**(22), 3736–3738 (2010).
11. J. W. Haus, G. Shaulov, E. A. Kuzin, and J. Sanchez-Mondragon, "Vector soliton fiber lasers," *Opt. Lett.* **24**(6), 376–378 (1999).
12. A. Martinez, M. Omura, M. Takiguchi, B. Xu, T. Kuga, T. Ishigure, and S. Yamashita, "Multi-solitons in a dispersion managed fiber laser using a carbon nanotube-coated taper fiber," in *Conference on Nonlinear Photonics (NP)*, Technical Digest (CD) (Optical Society of America, 2012) paper JT5A.29.
13. Y. S. Fedotov, S. M. Kobtsev, R. N. Arif, A. G. Rozhin, C. Mou, and S. K. Turitsyn, "Spectrum-, pulsewidth-, and wavelength-switchable all-fiber mode-locked Yb laser with fiber based birefringent filter," *Opt. Express* **20**(16), 17797–17805 (2012).
14. B. G. Bale, S. Boscolo, J. N. Kutz, and S. K. Turitsyn, "Intracavity dynamics in high-power mode-locked fiber lasers," *Phys. Rev. A* **81**(3), 033828 (2010).
15. Ph. Grelu and N. Akhmediev, "Dissipative solitons for mode-locked lasers," *Nat. Photonics* **6**(2), 84–92 (2012).
16. J. M. Soto-Crespo and N. Akhmediev, "Soliton as Strange Attractor: Nonlinear Synchronization and Chaos," *Phys. Rev. Lett.* **95**(2), 024101 (2005).
17. F. Li, P. K. A. Wai, and J. N. Kutz, "Geometrical description of the onset of multipulsing in mode-locked laser cavities," *J. Opt. Soc. Am. B* **27**(10), 2068–2077 (2010).
18. S. T. Cundiff, B. C. Collings, N. N. Akhmediev, J. M. Soto-Crespo, K. Bergman, and W. H. Knox, "Observation of polarization-locked vector solitons in an optical fiber," *Phys. Rev. Lett.* **82**(20), 3988–3991 (1999).
19. B. C. Collings, S. T. Cundiff, N. N. Akhmediev, J. M. Soto-Crespo, K. Bergman, and W. H. Knox, "Polarization-locked temporal vector solitons in a fiber laser: experiment," *J. Opt. Soc. Am. B* **17**(3), 354–365 (2000).
20. H. Zhang, D. Y. Tang, L. M. Zhao, and H. Y. Tam, "Induced solitons formed by cross-polarization coupling in a birefringent cavity fiber laser," *Opt. Lett.* **33**(20), 2317–2319 (2008).
21. L. M. Zhao, D. Y. Tang, X. Wu, H. Zhang, and H. Y. Tam, "Coexistence of polarization-locked and polarization-rotating vector solitons in a fiber laser with SESAM," *Opt. Lett.* **34**(20), 3059–3061 (2009).

22. L. M. Zhao, D. Y. Tang, H. Zhang, and X. Wu, "Polarization rotation locking of vector solitons in a fiber ring laser," *Opt. Express* **16**(14), 10053–10058 (2008).
 23. J. H. Wong, K. Wu, H. H. Liu, Ch. Ouyang, H. Wang, Sh. Aditya, P. Shum, S. Fu, E. J. R. Kelleher, A. Chernov, and E. D. Obraztsova, "Vector solitons in a laser passively mode-locked by single-wall carbon nanotubes," *Opt. Commun.* **284**(7), 2007–2011 (2011).
 24. D. Y. Tang, H. Zhang, L. M. Zhao, and X. Wu, "Observation of high-order polarization-locked vector solitons in a fiber laser," *Phys. Rev. Lett.* **101**(15), 153904 (2008).
 25. C. Mou, S. Sergeyev, A. Rozhin, and S. Turistyn, "All-fiber polarization locked vector soliton laser using carbon nanotubes," *Opt. Lett.* **36**(19), 3831–3833 (2011).
 26. C. Mou, S. Sergeyev, A. Rozhin, and S. K. Turitsyn, "Vector Solitons with Slowly Precessing States of Polarization," in *Conference on Nonlinear Photonics (NP)*, Technical Digest (CD) (Optical Society of America, 2012) paper NTu2D.
 27. D. G. Aronson, G. B. Ermentrout, and N. Kopell, "Amplitude response of coupled oscillators," *Physica D* **41**(3), 403–449 (1990).
-

1. Introduction

Polarization dynamics in lasers (including gas, solid state, semiconductor, dye and fiber lasers) have been intensively studied for more than two decades in the context of various applications in fiber optic communication, fiber optic sensors, material processing (cutting, welding etc.) and nanophotonics (manipulation of asymmetric particles) [1–4]. In such systems two laser modes with the same longitudinal and transverse spatial patterns and different polarization states, frequencies, and amplitudes interact through the gain sharing, phase- and amplitude selective nonlinear processes (Kerr nonlinearity) and in-cavity components (polarizers, polarization controllers etc.). As a result of the interaction, different polarization patterns have been found including polarization chaos [5–10]. In fiber lasers, due to long cavity length and wide gain bandwidth, typically, a large number of modes are generated. This leads to stochastic polarization dynamics as a result of spontaneous mode-locking [9, 10]. However, implementation of passive or active mode-locking techniques results in suppression of stochastic dynamics and so regular dynamics in the form of dissipative solitons were observed [11–26]. Dynamics and stability of solitons on a longer time scale (at the level of thousands of cavity round trips) is well governed by round trip-based Poincaré mapping [14] and the corresponding theory of dynamical systems leading to different "attractors" (fixed point, periodic, quasi-periodic, chaotic) [15–17]. The vectorial nature of the DSs has been observed in Fast Polarization Rotating or Locked Vector Solitons (PRVS and PLVS) [18–26]. In PLVS pulses are locked to a fixed elliptically polarized state [18–21, 24, 25] while PRVSs have demonstrated different types of anti-phase dynamics for cross polarized SOPs with a period of a few round trips [21–23]. Note that information about the phase difference between orthogonal SOP was missed and so observed polarization dynamics of VS's can't be related to any polarization attractor. In our previous papers, we have experimentally characterized polarization attractors in erbium doped fiber laser mode locked with carbon nanotubes [25, 26]. In a fundamental soliton operation, we have found polarization attractors in the form of fixed point, single and double semi-circles on the surface of the Poincaré sphere [25, 26].

In this work we report to the best of our knowledge a first complete experimental characterization of new families of vector solitons in a carbon nanotube mode-locked fiber laser with anomalous dispersion laser cavity. Experimental data has been collected using an in-line polarimeter. By tuning an in-cavity polarization controller (POC) and POC for the pump laser (Fig. 1), we have found a new type of vector solitons with locked and precessing SOPs for fundamental soliton and multipulsing operations on a time scale of 40–40000 round-trips. The observed polarization attractors might be a key to the future enabling technologies of secure communications [1], trapping and manipulation of atoms and nanoparticles [2, 3] and vectorial control of magnetization [4].

2. Experimental set-up and results

The experimental setup is shown in Fig. 1. The ring cavity fiber laser with a total length of 7.83m comprises 2 m of high concentration erbium doped fiber (LIEKKI™ Er80-8/125) and

single mode (SM) fiber with anomalous dispersion (group velocity dispersion (GVD) parameter for erbium fiber $\beta_{2,EDF} = -19.26 \text{ fs}^2 / \text{mm}$), polarization controllers (POCs), wavelength division multiplexing (WDM) coupler, optical isolator (OIS) to provide unidirectional lasing, saturable absorber (polymer film with carbon nanotubes (CNT)), and output coupler. The CNT mode-locker is embedded between two standard fiber connector ferrules and index matching gel is applied to minimize the transmission loss. The cavity is pumped via 980/1550 WDM by a 976 nm laser diode (LD) with a maximum current of about 355 mA which provides 170 mW of optical power. With the help of a 90:10 coupler 90% of the intracavity power was directed out of the cavity. Output lasing has been analyzed with help of an auto-correlator (Pulsecheck), oscilloscope (Tektronix), optical spectrum analyzer (ANDO AQ6317B) and in-line polarimeter (Thorlabs, IPM5300).

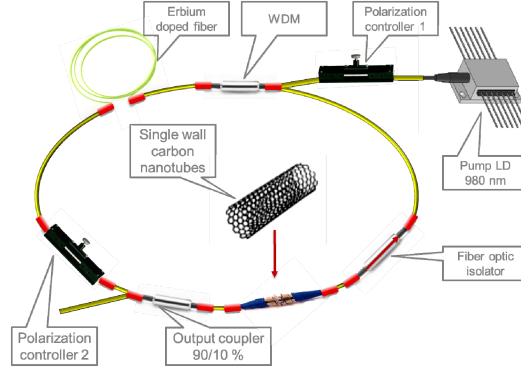


Fig. 1. Experimental set-up

The polarimeter with 1 μs resolution and interval of 1 ms (40 – 40000 round trips) measures normalized Stokes parameters s_1 , s_2 , s_3 and degree of polarization DOP which are related to the output powers of two linearly cross-polarized SOPs $|u|^2$ and $|v|^2$, and phase difference between them $\Delta\varphi$ as follows:

$$S_0 = |u|^2 + |v|^2, S_1 = |u|^2 - |v|^2, S_2 = 2|u||v|\cos\Delta\varphi, S_3 = 2|u||v|\sin\Delta\varphi,$$

$$s_i = \frac{S_i}{\sqrt{S_1^2 + S_2^2 + S_3^2}}, DOP = \frac{\sqrt{S_1^2 + S_2^2 + S_3^2}}{S_0}, (i=1,2,3). \quad (1)$$

In the experiment, pump current has been changed from 209 mA to 355 mA and the in-cavity polarization and pump polarization controller have been tuned to obtain the polarization attractors shown in Figs. 2-5. In view of auto-correlator sensitivity to the input SOP, all auto-correlation traces have been averaged over 16 samples.

The experimental results for the pump current of 209 mA are shown in Fig. 2(a-f). The output optical spectrum shown in Fig. 2(a) is centered at 1560 nm and the Kelly sidebands indicate the fundamental soliton shape of the output pulses. A typical pulse train shown in Fig. 2(b) has period $T = 38.9 \text{ ns}$ and so a repetition rate of 25.7 MHz. The fundamental soliton shape of $\text{sech}^2(t/T_p)$ matches the measured autocorrelation trace with the pulse width $T_p = 455 \text{ fs}$ (Fig. 2(c)). By rotating in-cavity POC we increase the cavity's anisotropy and so we observed a vector soliton locked nearby the linearly polarized SOP at the surface of the Poincaré sphere (Fig. 2(d-e)). Output power of the observed PLVS is 0.15 mW, phase difference $\Delta\varphi \approx \pi$ and $DOP = 61\%$. Thus, the PLVS shown in Fig. 1 can be related to the polarization attractor at the Poincaré sphere in the form of a fixed point.

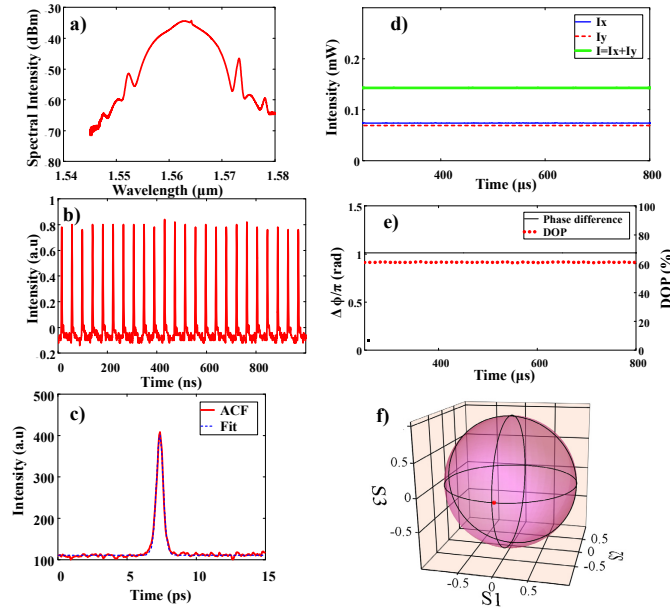


Fig. 2. Polarization locked vector soliton. (a) output optical spectrum, (b) single pulse train, (c) measured auto-correlation trace. Polarization dynamics in the time frame of 40-40 000 round trips ($1 \mu\text{s} - 1 \text{ms}$) in terms of (d) optical power of orthogonally polarized modes I_x (solid line) and I_y (dashed line), total power $I = I_x + I_y$ (dotted line), (e) phase difference and degree of polarization, and (f) Stokes parameters at Poincaré sphere. Parameters: pump current $I_p = 209$, mA, period $T = 38.9$ ns, pulse width $T_p = 455$ fs, output power $I = 0.15$ mW, phase difference $\Delta\phi \approx \pi$ and $DOP = 61\%$.

With pump current increased to 306 mA, multi-pulsing was observed (Fig. 3). The multi-pulsing arises as a result of interplay between the laser cavities' bandwidth constraints and the energy quantization associated with the resulting mode-locked pulses [17]. The mode-locked pulse has increasing peak power and spectral bandwidth with increased pump power. However, the increase in the mode-locked spectral bandwidth is limited by the gain bandwidth of the cavity. To overcome this constraint with further increasing the pump power, a single pulse is split into two pulses per round trip with energy divided between two pulses and spectral bandwidths within the gain bandwidth window. As a result, double pulsing with the period $T = 38.9$ ns, pulse width $T_p = 247$ fs, and output power $I \approx 0.55$ mW has been observed (Fig. 3(a-d)). Anti-phase dynamics of oscillations for two cross polarized SOPs results in cw operation for the total output power (Fig. 3(d)). DOP oscillations around a low value of 12% indicate the presence of SOP oscillations faster than the polarimeter resolution time of $1 \mu\text{s}$ (Fig. 3(e)). The trace of the fast oscillations can be found in Fig. 3(e) as fast phase difference jumps and so the resulting polarization attractor at the Poincaré sphere comprises a polyline winding around a circle (Fig. 3(f)). This attractor is located close to the left circularly polarized SOP which is an eigenstate for isotropic laser along with the right circularly polarized SOP and all linearly polarized SOPs (equator at the Poincaré sphere) [5].

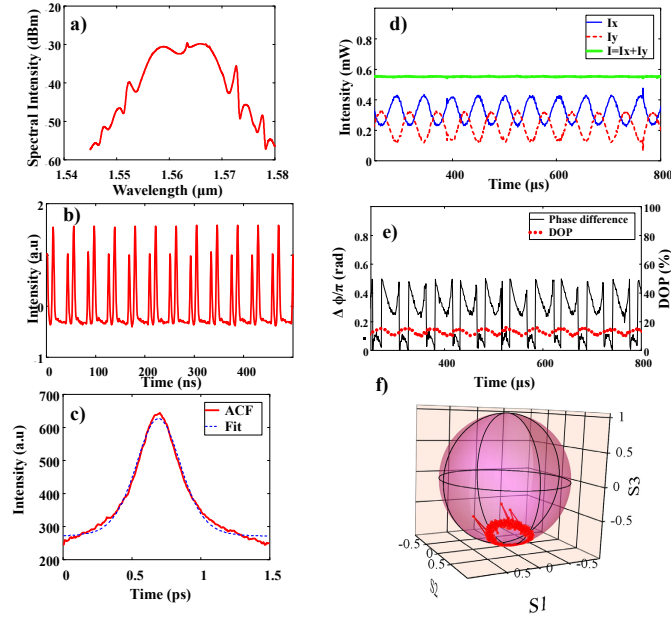


Fig. 3. Vector soliton with slowly evolving state of polarization for two-pulse operation. (a) output optical spectrum, (b) single pulse train, (c) measured auto-correlation trace. Polarization dynamics in the time frame of 40-40 000 round trips ($1 \mu\text{s} - 1 \text{ms}$) in terms of (d) optical power of orthogonally polarized modes I_x (solid line) and I_y (dashed line), total power $I = I_x + I_y$ (dotted line), (e) phase difference and degree of polarization, and (f) Stokes parameters at Poincaré sphere. Parameters: pump current $I_p = 306 \text{ mA}$, period $T = 38.9 \text{ ns}$, pulse width $T_p = 247 \text{ fs}$, output power $I \approx 0.55 \text{ mW}$.

Further pump power current increase up to 320 mA results in five-pulse soliton dynamics with with period $T = 38.9 \text{ ns}$, pulse width $T_p = 292 \text{ fs}$, output power $I \approx 0.65 \text{ mW}$ (Fig. 4(a-d)). As follows from Fig. 4(c), output laser SOP is changing fast and so averaging over 16 samples is not enough to obtain smooth fundamental soliton shape of the autocorrelation trace. Anti-phase dynamics of oscillations for two cross polarized SOPs results in weak periodic oscillations of the total output power (Fig. 4(d)). As compared to Fig. 3, DOP is oscillating around the higher value of 30% that also indicates the presence of SOP oscillations faster than polarimeter resolution time of $1 \mu\text{s}$ (Fig. 4(e)). The trace of the fast oscillations can be also found in the phase difference dynamics shown in Fig. 4(e). As a result of the fast phase jumps between cross polarized SOPs and slow SOP precessing, the polarization attractor at the Poincaré sphere comprises a polyline with an outline in the form of a circle (Fig. 4(f)). This attractor is located close to the equator at the Poincaré sphere which is an eigenstate for an isotropic laser [5].

With a pump current increased to 355 mA , output dynamics takes the form of a two-pulse harmonic mode-locking operation (Fig. 5(a-d)) with period $T = 20 \text{ ns}$, pulse width $T_p = 228 \text{ fs}$, output power $I \approx 0.8 \text{ mW}$ (Fig. 4(a-d)). Anti-phase dynamics of the output power of two-cross polarized modes result in operation of the total output power close to cw (Fig. 5(d)). DOP and phase difference are almost stabilized and so weak oscillation has been observed around 30% and 0.2π (Fig. 5(e)). Thus, the vector soliton shown in Fig. 5 can be related to the polarization attractor at the Poincaré sphere in the form of a limit cycle (Fig. 5(f)). In view of the unequal powers for two cross-polarized SOPs, this attractor corresponds to the case of a strong anisotropy created by in-cavity POC.

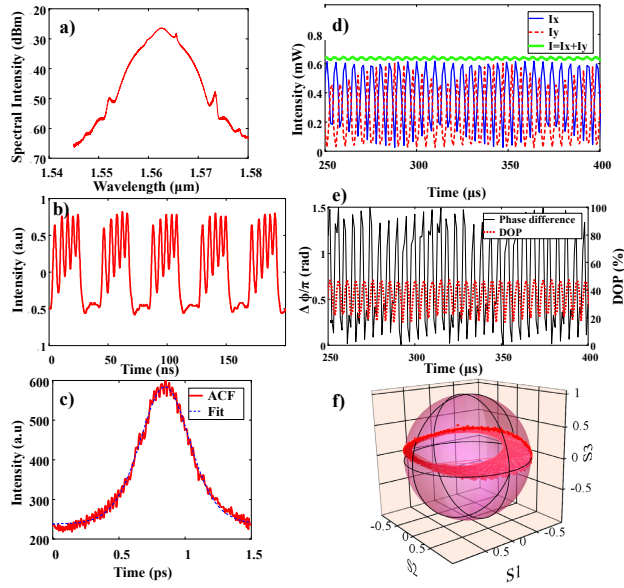


Fig. 4. Vector soliton with slowly evolving state of polarization for five-pulse operation. (a) output optical spectrum, (b) single pulse train, (c) measured auto-correlation trace. Polarization dynamics in the time frame of 40-40 000 round trips ($1 \mu\text{s} - 1 \text{ms}$) in terms of (d) optical power of orthogonally polarized modes I_x (solid line) and I_y (dashed line), total power $I = I_x + I_y$ (dotted line), (e) phase difference and degree of polarization, and (f) Stokes parameters at Poincaré sphere. Parameters: pump current $I_p = 320 \text{ mA}$, period $T = 38.9 \text{ ns}$, pulse width $T_p = 292 \text{ fs}$, output power $I \approx 0.65 \text{ mW}$.

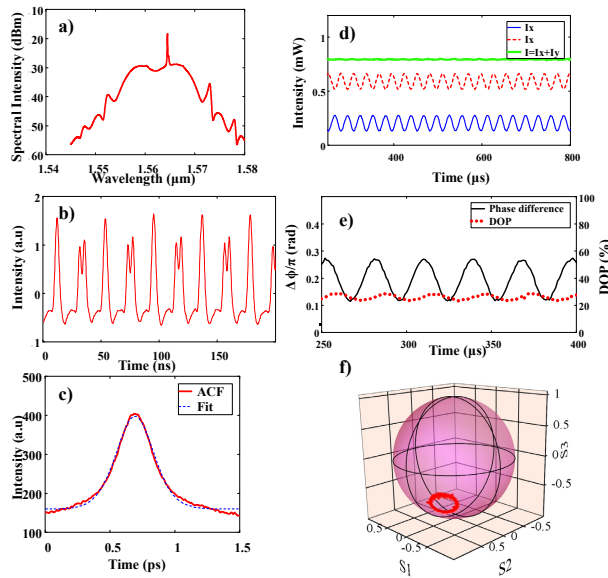


Fig. 5. Vector soliton with slowly evolving state of polarization for two-pulse operation. (a) output optical spectrum, (b) single pulse train, (c) measured auto-correlation trace. Polarization dynamics in the time frame of 40-40 000 round trips ($1 \mu\text{s} - 1 \text{ms}$) in terms of (d) optical power of orthogonally polarized modes I_x (solid line) and I_y (dashed line), total power $I = I_x + I_y$ (dotted line), (e) phase difference and degree of polarization, and (f) Stokes parameters at Poincaré sphere. Parameters: pump current $I_p = 355 \text{ mA}$, period $T = 20 \text{ ns}$, pulse width $T_p = 228 \text{ fs}$, output power $I \approx 0.55 \text{ mW}$.

As follows from Figs. 2-5, phase difference dynamics indicate the presence of coherent coupling between cross-polarized SOPs through the gain sharing and pump and in-cavity polarization controllers similar to the polarization dynamics of single- and multi-mode lasers without a saturable absorber [5–10]. It is well known from the theory of nonlinear coupled oscillators that weak coupling leads to a complex behavior, and increasing the coupling leads to stabilization of the behavior, i.e. coupled attractors approach a stable steady state [27]. The coupling is determined by pump power, amplitude and phase anisotropy of the cavity caused by polarization controllers. Complex polarization attractors in Figs. 3 and 4 are the result of a weak coupling caused by isotropic cavity. Stabilization takes place with an increased amplitude and phase anisotropy in the cavity and leads to the more simple attractors in the form of the fixed point and the limit cycle (Figs. 2 and 5).

4. Conclusions

Using an in-line polarimeter for erbium doped fiber laser passively mode locked with carbon nanotubes, we demonstrated for the first time new types of vector solitons with locked and slowly evolving states of polarization on a time scale of 40-40000 round-trips for fundamental soliton and multipulsing operations. The obtained results can find a practical implementation in secure communications [1], trapping and manipulation of atoms and nanoparticles [2, 3] and vectorial control of magnetization [4].

Acknowledgment

S. Sergeyev acknowledges financial support from the European Union program FP7 PEOPLE-2009-IEF (grant 253297). The work was also supported by the European Research Council, the Leverhulme Trust, FP7 Marie Curie project IRSES, and the grant N11.519.11.6038 of the Ministry of Education and Science of the Russian Federation.